HNPS Advances in Nuclear Physics

Vol 12 (2003)

HNPS2003

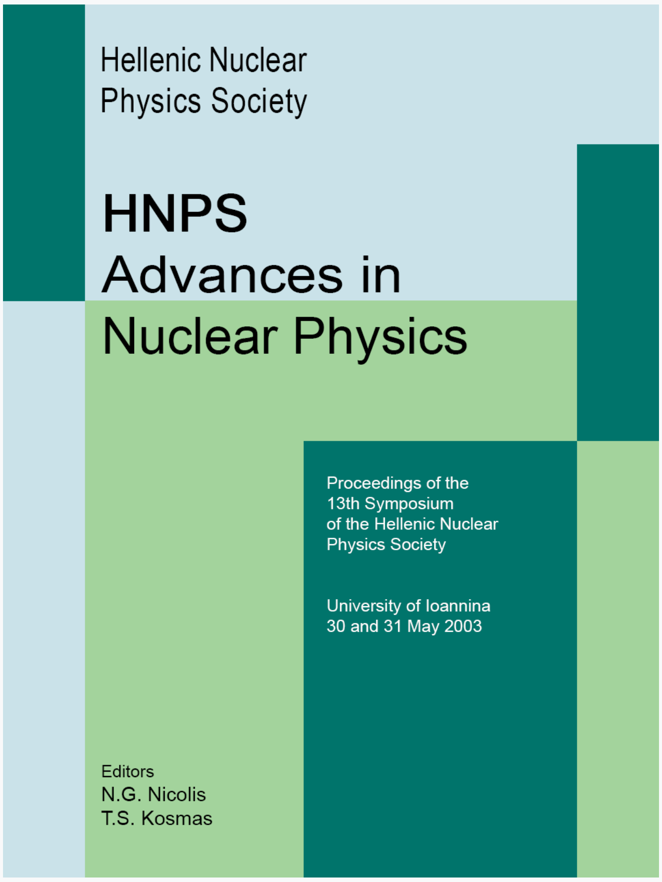

Hellenic Nuclear
Physics Society

HNPS
Advances in
Nuclear Physics

Proceedings of the
13th Symposium
of the Hellenic Nuclear
Physics Society

University of Ioannina
30 and 31 May 2003

Editors
N.G. Nicolis
T.S. Kosmas

Metals, the plasma of the poor man?

C. Rolfs

doi: 10.12681/hnps.3342

To cite this article:

Rolfs, C. (2021). Metals, the plasma of the poor man?. *HNPS Advances in Nuclear Physics*, *12*, 16–27. https://doi.org/10.12681/hnps.3342

https://epublishing.ekt.gr | **e-Publisher:** EKT | **Downloaded at:** 10/05/2026 18:50:24

HNPS Advances in Nuclear Physics vol. 12, pp. 16-27 (2003)
C. Rolfs HNPS2003 doi:10.12681/hnps.3342

Metals, the plasma of the poor man ?

C.Rolfs
Institut für Physik mit Ionenstrahlen, Ruhr-Universität Bochum, Germany

Abstract: The electron screening effect in the d(d,p)t reaction has been studied for deuterated metals, insulators, and semiconductors, i.e. 58 samples in total. As compared to measurements performed with a gaseous D_2 target, a large effect has been observed in most metals, while a small (gaseous) effect is found e.g. for the insulators, semiconductors, and lanthanides. The periodic table provides the ordering of the observed small and large effects in the samples. An explanation of the large effects in metals is possibly provided by the classical plasma screening of Debye applied to the quasi-free metallic electrons. The data also provide information on the solubility of hydrogen in the samples.

1. Introduction

It is well known that the cross section $\sigma(E)$ of a charged-particle-induced nuclear reaction is enhanced at low energies by the electron clouds surrounding the interacting nuclides, with an enhancement factor [1-4]

$$f_{lab}(E) = E\,(E+U_e)^{-1} \exp(-2\pi\eta(E+U_e)+2\pi\eta(E)), \quad \text{for } S(E+U_e) \approx S(E) \qquad (1)$$

where $\eta(E)$ is the Sommerfeld parameter, S(E) the astrophysical S-factor, and U_e the screening potential energy. In the adiabatic limit, U_e can be calculated from the difference in atomic binding energies between the compound atom and the projectile plus target atoms of the entrance channel or from the Coulomb energy of the electron cloud at some atomic radius. For the d(d,p)t reaction the adiabatic limit is U_{ad} = 39 eV for neutral atoms and 52 eV, if the projectile is a positively charged ion at the moment of interaction; from the Coulomb energy of the H atom one expects U_e = 2x13.6 eV = 27.2 eV.

The screening effect in d(d,p)t has been studied previously for 6 deuterated metals [5,6], where the resulting S(E) data showed for 4 metals an exponential enhancement according to equation 1. However, the extracted U_e values (190 to 600 eV) were about one order of magnitude larger than the value found in a gas-target experiment: U_e = 25±5 eV [7]. Our study of deuterated Ta led to U_e = 340±14 eV [8,9] confirming the previous observation [5]. Recently, we reported on preliminary results for several metals, insulators, and semiconductors [9,10]. The present report completes these investigations superseding the preliminary results.

2. Experimental procedures

The equipment, procedures, and data analysis have been described elsewhere [8]. Briefly, the 100 kV accelerator of the Dynamitron-Tandem-Laboratorium at the Ruhr-Universität Bochum provided the deuteron beam. A liquid-nitrogen-cooled Cu tube extended to within 5 cm of the target. Four Si detectors were installed at an angle $\theta = 130^\circ$ around the beam axis at a 5 cm distance from the target and covered with a Ni foil to stop the intense flux of elastically scattered particles. The target together with the chamber and the detector holders (including the Ni foils) formed a Faraday cup for beam integration. A negative voltage of 200 V was applied to the Cu tube for suppression of secondary electrons.

Each deuterated target was produced in the following way. A fresh polycristalline material “M” was bombarded with 10 keV deuterons, whereby the proton yield of d(d,p)t was recorded as a function of implantation charge: the yield reached usually a saturation level after a charge of about 1 C, i.e. a stoichiometry M_xD has been produced near the surface of the target, where $1/x$ = “D/M” corresponds to the solubility of hydrogen in the sample. The procedure was repeated at higher deuteron energies. The deuteron distribution was investigated subsequently via Elastic-Recoil-Detection-Analysis at the 4 MV tandem accelerator in Bochum. For most of the materials the distribution was uniform within 10% from the surface down to a depth consistent with the range of the implanted deuterons.

The reaction yield of the infinitely thick target, $Y^\infty(E_d,\theta)$, was obtained in several runs at E_d = 5 to 30 keV, with energy steps ΔE_d of 0.5 keV at E_d = 5 to 10 keV and 1.0 keV at E_d = 10 to 30 keV. In order to arrive at a thin-target yield curve, $Y(E_d,\theta)$, the thick-target yield curve was differentiated, i.e. the yield difference between two adjacent points $Y^\infty(E_d,\theta)$ and $Y^\infty(E_d-\Delta E_d,\theta)$ was calculated and divided by ΔE_d. The energy steps ΔE_d correspond to about 50 and 100 monolayers near the surface. The result is

$$Y(E_d,\theta) = \alpha \; \varepsilon_{eff}(E_d)^{-1} \, \sigma(E_{eff}) \,, \tag{2}$$

with the effective energy E_{eff} [1] and the constant α, as measured using a radioactive source [8]. The effective stopping power $\varepsilon_{eff}(E_d)$ for the M_xD target is given by the expression

$$\varepsilon_{eff}(E_d) = \varepsilon_D(E_d) + x \, \varepsilon_M(E_d). \tag{3}$$

From the compilation SRIM [11] one finds that the energy dependence of $\varepsilon_{eff}(E_d)$ at E_d = 5 to 30 keV is identical with $\varepsilon_M(E_d)$ to within 5% for a wide range of x values, mainly due to the velocity-proportional stopping power and the feature $\varepsilon_M(E_d) >> \varepsilon_D(E_d)$; thus, the deduced energy dependence of $\sigma(E_{eff})$ is nearly independent from the stoichiometric ratio x.

Subsequent Rutherford-Backscattering-Spectrometry of the samples exhibited no detectable surface contamination except for Al which revealed an Al_2O_3 surface layer with a thickness of about 150 monolayers. Since this thickness is larger than the energy step in our differentiation method, the reported $U_e \leq 30$ eV value [9] corresponded to the case of an Al_2O_3 insulator and not to an Al metal (Table 1). Since Al oxides rapidly in air, we cleaned the Al surface *in situ* by Kr sputtering at 15 keV (at the 100 kV accelerator) removing at least 100 monolayers. After this cleaning the above experimental procedure was carried out leading to $U_e = 520\pm50$ eV for the metal Al (Table 1). This surface cleaning by Kr sputtering was carried out subsequently as a first step in the experimental procedures, for each new sample as well as for all of the previously studied samples [9,10], where the target temperature was always $T = 20^oC$; in particular, the noble metals Cu, Ag, and Au exhibited - after this cleaning procedure - also a large enhancement effect.

The resulting cross section $\sigma(E_{eff})$, i.e. the weighted average of several runs, is illustrated in Fig. 1 in form of the astrophysical S(E) factor for the examples Cu, Nd, Hf, and Pt and numerical values for all the samples can be found in [12]. The errors shown in Fig. 1 arise predominantly from the spread of the (differentiated thick-target) thin-target yields from various runs. The absolute scale was obtained by normalisation to previous work [7] at $E_d = 30$ keV including the effects of electron screening where applicable. The normalisation led to a value for the stoichiometric ratio x given in Table 1 in form of the hydrogen solubility 1/x.

In the analysis of the data (e.g. Fig. 1) we assumed a bare S(E) factor (i.e. for bare interacting nuclides) linearly increasing with energy, $S_b(E) = 43 + 0.54$ E [keV b] (center-of-mass energy E in keV), as found previously [7,8]. Relative to this function, the data were fitted with the enhancement factor of equation 1: the resulting U_e values are summarized in Table 1.

It should be pointed out that the quoted U_e values rely on the energy dependence of the stopping power values of deuterons in the metals at energies far below the Bragg peak, where no energy loss data exist and the values derived from the compilation SRIM [11] are based on extrapolations. However, recent measurements of low-energy stopping powers of protons in C, Al, Ni, and Au [13] have confirmed the SRIM extrapolations. Additional measurements of low-energy stopping powers are highly desirable for an improved determination of U_e, where the quoted errors in Table 1 contain yet no systematic uncertainty in the stopping power values.

In one experiment, we increased the target temperature to $T = 100^oC$ using diffilen oil supplied by a cryo-circulator (JULABO FP90), whereby a thermoelement had been placed behind the target to measure T with a precision of 2^oC (including beam-heating effects). For deuterated Pt we find U_e = 530±40 eV (with 1/x = 0.06) showing a decrease of U_e with increasing T (for T = 20°C: U_e = 670±50 eV, 1/x = 0.06; Table 1).

In another experiment, we used a deuterated Pt target and a ^{3}He ion beam in combination with the reaction d(^{3}He,p)^{4}He to study the associated electron screening effect; here we have $S_b(E)$ = 6.7 + 0.0243 E [MeV b], with center-of-mass energy E in keV ([3] and references therein). The result is U_e = 680±60 eV showing that high U_e values do not depend on the kind of ion species but are a feature of the deuterated metals.

3. Discussion

A comparison of the U_e values with the periodic table indicates a common feature (Fig. 2): for each group of the periodic table, the corresponding U_e values are either low ("gaseous") as for groups 3 and 4 and the lanthanides, or high such as for the groups 2, 5 to 12, and 15. Group 14 is an apparent exception to this feature: the metals Sn and Pb have a high U_e value, while the semiconductors C, Si, and Ge have a low U_e value indicating that high U_e values are a feature of metals. A similar situation is found for group 13: B = insulator, Al and Tl = metals. The indication is supported further by the insulators BeO, Al_2O_3, and CaO_2. The deuterated metals of groups 3 and 4 and the lanthanides have a high hydrogen solubility, of the order of one, and thus represent also insulators; their observed solubilities are consistent with previous work [14]. For the metals with high U_e values, the solubilities are reported to be quite small, but actual values at room temperature are not available except for a few cases; the present work leads to solubilities of about 12% on average leaving the metallic character of the samples essentially unchanged.

Since the data for all metals with large U_e values could be fitted well with equation 1, the enhanced cross section is most likely due to electron effects of the environment of the target deuterons. Various aspects of the metals were discussed previously to explain possibly the data [8,9]: stopping power, thermal motion, channeling, diffusion, conductivity, crystal structure, electron configuration, and "Fermi shuttle" acceleration mechanism; however, none of these aspects led to a solution.

If n_{eff} is the number of valence electrons per metallic atom which can be effectively treated as classical and quasi-free, one may apply the classical plasma theory of Debye leading to an electron sphere of radius [1,15]

$$R_D = (\varepsilon_o kT / e^2 n_{eff} \rho_a)^{1/2} = 69 (T / n_{eff} \rho_a)^{1/2} \quad [m] \qquad (4)$$

around positive singly-charged ions (here: deuterons in the lattice) with the temperature of the free electrons T in units of K and the atomic density ρ_a in units of m^{-3}. For T = 293 K, ρ_a =

6x10^{28} m^{-3}, and n_{eff} = 1 one obtains a radius R_D, which is about a factor 10 smaller than the Bohr radius of a hydrogen atom. With the Coulomb energy between two deuterons at R_D set equal to U_e, one obtains $U_e = (4\pi\varepsilon_o)^{-1} e^2/R_D$ = 300 eV, the order of magnitude of the observed U_e values. A comparison of the calculated and observed U_e values leads to n_{eff} given in Table 1: for most metals n_{eff} is of the order of one. The acceleration mechanisms of the incident ions leading to the high observed U_e values is thus – within our simple model - the Debye electron cloud at the rather small radius R_D.

A critical test of the classical Debye model is the predicted temperature dependence, $U_e \propto T^{-1/2}$. For deuterated Pt we find a ratio $R_{exp} = U_e(100^oC) / U_e(20^oC)$ = 0.79±08, in fair agreement with the expected value R_{theo} = 0.88±0.01 from our model. If one includes the observed 8±2% decrease of n_{eff} over this temperature range (see below), the agreement is somewhat better (R_{theo} = 0.84±0.02).

The observed U_e values for the d(d,p)t and d(^{3}He,p)^{4}He reactions in deuterated Pt are identical within experimental uncertainties (d^+-beam: U_e = 670±50 eV; $^3He^+$-beam: U_e = 680±60 eV). For the singly charged ions used in the experiment, one expects the U_e values – according to the above model - to be indeed identical.

An alternative determination of n_{eff} is obtained from the observed Hall coefficient for metals at room temperature ([16] and references therein),

$$C_{Hall} = (e\ n_{eff}(Hall)\ \rho_a)^{-1}, \qquad (5)$$

where for about 50% of the metals in Table 1 the coefficient is negative (electron carriers) and for the other one-half it is positive (hole carriers). Since in the latter case essentially also electrons move (however in the opposite direction), we assumed that any dependence on the + or – sign of C_{Hall} can be neglected (which needs theoretical verification). The resulting n_{eff}(Hall) values are also given in Table 1: there is a remarkable correlation between n_{eff} and n_{eff}(Hall) both for electron and hole carriers, i.e. within 2 standard deviations the two quantities agree for all metals with a known Hall coefficient, except for Pd and Ir. Our own measurement of the Hall coefficient for Pd led [12] to n_{eff}(Hall) = 3.4±0.7 removing essentially the discrepancy with n_{eff} = 6.3±1.3. Thus, it appears desirable to measure or remeasure the Hall coefficient for all metals with a high U_e value (Table 1).

Although the classical Debye model appears to explain to a large extent the data, it is well known that most of the conduction electrons are not classical but are frozen by quantum effects and only electrons close to the Fermi energy (E_F) actually should contribute to screening. A standard calculation of a Fermi gas at low temperature ($kT << E_F$) yields an effective number $n_{eff}(Fermi) = 0.67\ kT/E_F$ and correspondingly the screening potential energy U_e should be about

10 eV at room temperature (for $E_F = 3$ eV). However, near room temperature the Hall coefficient C_{Hall} is observed for many metals to increase with temperature [16], e.g. for Pt by 8% between T = 20°C and 100°C, while from n_{eff}(Fermi) one expects a decrease for C_{Hall} by 34% over this temperature range. Furthermore, inserting n_{eff}(Fermi) into equation 4, one expects no temperature dependence for U_e, in conflict with our observation. Thus, the data for the electron screening as well as for the Hall coefficient suggest some deviation from this simple however well established treatment of conduction electrons.

1. C.Rolfs, W.S.Rodney: Cauldrons in the cosmos (University of Chicago Press, 1988)
2. H.J.Assenbaum, K.Langanke, C.Rolfs: Z. Phys. A327(1987)461
3. F.Strieder et al.: Naturwissenschaften 88(2001)461
4. L.Bracci et al.: Nucl. Phys. A513(1990)316
5. K.Czerski et al.: Europhys. Lett. 54(2001)449
6. H.Yuki et al.: JETP Lett. 68(1998)823
7. U.Greife et al.: Z. Phys. A351(1995)107
8. F.Raiola et al.: Eur. Phys. J. A13(2002)377
9. F.Raiola et al.: Conference Proc. *Nuclear Physics in Astrophysics* (Debrecen, October 2002), Nucl.Phys. A719(2003)
10. F. Raoila et al., Eur. Phys. J A19, 283 (2004)
11. H.Andersen, J.F.Ziegler: The stopping and ranges of ions in matter (Pergamon, New York, 1977) and SRIM-2000/2003
12. F.Raiola: Thesis, Ruhr-Universität Bochum (2003); C.Bonomo: Tesi di Laurea, University of Catania (2003)
13. S.P.Møller et al.: Phys. Rev. Lett. 88(2002)193201
14. W.M.Mueller, J.P.Blackedge, G.G.Libowitz: Metal Hydrides (Academic Press, New York, 1968); F.A.Lewis, A.Aladjem: Hydrogen Metal Systems (Solid State Phenomena, Vol. 49-50, Scitec Publ., Zürich, 1996)
15. F.F.Chen: Introduction to plasma physics and controlled fusion (Plenum, New York, 1984)
16. Landolt-Börnstein, Vol. II.6 (Springer, Berlin, 1959); C.M.Hurd: The Hall effect in metals and alloys (Plenum Press, 1972)

Fig. 1: Astrophysical S(E) factor of the reaction d(d,p)t as obtained for the deuterated samples Cu, Nd, Hf, and Pt (E = effective center-of-mass energy). The dotted curve represents the bare

S(E) factor, while the solid curve includes the exponential enhancement due to electron screening with the U_e value given.

Fig. 2: Periodic table showing the studied elements, where those with low U_e values ($U_e < 100$ eV, small effect) are lightly shadowed and those with high U_e values ($U_e \geq 100$ eV, large effect) are heavily shadowed.

Table 1: summary of results[a]

material	U_e (eV)[b]	solubility $1/x$[c]	n_{eff} [b]	n_{eff}(Hall)[d]
metals				
Be	180±40	0.08	0.2±0.1	(0.21±0.04)
Mg	440±40	0.11	3.0±0.5	1.8±0.4
Al	520±50	0.26	3.0±0.6	3.1±0.6
V	480±60	0.04	2.1±0.5	(1.1±0.2)
Cr	320±70	0.15	0.8±0.4	(0.20±0.04)
Mn	390±50	0.12	1.2±0.3	(0.8±0.2)
Fe	460±60	0.06	1.7±0.4	(3.0±0.6)
Co	640±70	0.14	3.1±0.7	(1.7±0.3)
Ni	380±40	0.13	1.1±0.2	1.1±0.2
Cu	470±50	0.09	1.8±0.4	1.5±0.3
Zn	480±50	0.13	2.4±0.5	(1.5±0.3)
Sr	210±30	0.27	1.7±0.5	
Nb	470±60	0.13	2.7±0.7	(1.3±0.3)
Mo	420±50	0.12	1.9±0.5	(0.8±0.2)
Ru	215±30	0.18	0.4±0.1	(0.4±0.1)
Rh	230±40	0.09	0.5±0.2	(1.7±0.4)
Pd	800±90	0.03	6.3±1.3	1.1±0.2
Ag	330±40	0.14	1.3±0.3	1.2±0.3
Cd	360±40	0.18	1.9±0.4	(2.5±0.5)
In	520±50	0.02	4.8±0.9	
Sn	130±20	0.08	0.3±0.1	
Sb	720±70	0.13	11±2	
Ba	490±70	0.21	9.9±2.9	
Ta	270±30	0.13	0.9±0.2	(1.1±0.2)
W	250±30	0.29	0.7±0.2	(0.8±0.2)
Re	230±30	0.14	0.5±0.1	(0.3±0.1)
Ir	200±40	0.23	0.4±0.2	(2.2±0.5)
Pt	670±50	0.06	4.6±0.7	3.9±0.8
Au	280±50	0.18	0.9±0.3	1.5±0.3
Tl	550±90	0.01	5.8±1.2	(7.4±1.5)
Pb	480±50	0.04	4.3±0.9	
Bi	540±60	0.12	6.9±1.5	
semiconductors				
C	≤60	0.35		
Si	≤60	0.23		
Ge	≤80	0.56		
insulators				
BeO	≤30	0.25		
B	≤30	0.38		
Al_2O_3	≤30	0.27		
CaO_2	≤50	0.60		
groups 3 and 4				
Sc	≤30	1.4		
Ti	≤30	1.3		
Y	≤70	1.8		
Zr	≤40	1.1		
Lu	≤40	1.5		
Hf	≤30	1.8		
lanthanides				
La	≤60	0.6		
Ce	≤30	1.3		
Pr	≤70	0.9		

Nd	≤30	0.7
Sm	≤30	1.3
Eu	≤50	0.6
Gd	≤50	1.4
Tb	≤30	1.3
Dy	≤30	1.1
Ho	≤70	1.6
Er	≤50	1.0
Tm	≤70	1.4
Yb	≤ 40	1.3

---

[a] For a target temperature of T = 20°C and a surface cleaning by Kr sputtering

[b] Error contains no systematic uncertainty in stopping power

[c] Estimated uncertainty is about 20%

[d] From the observed Hall coefficient at T = 20°C [16], with an assumed 20% error; the numbers in brackets are for hole carriers

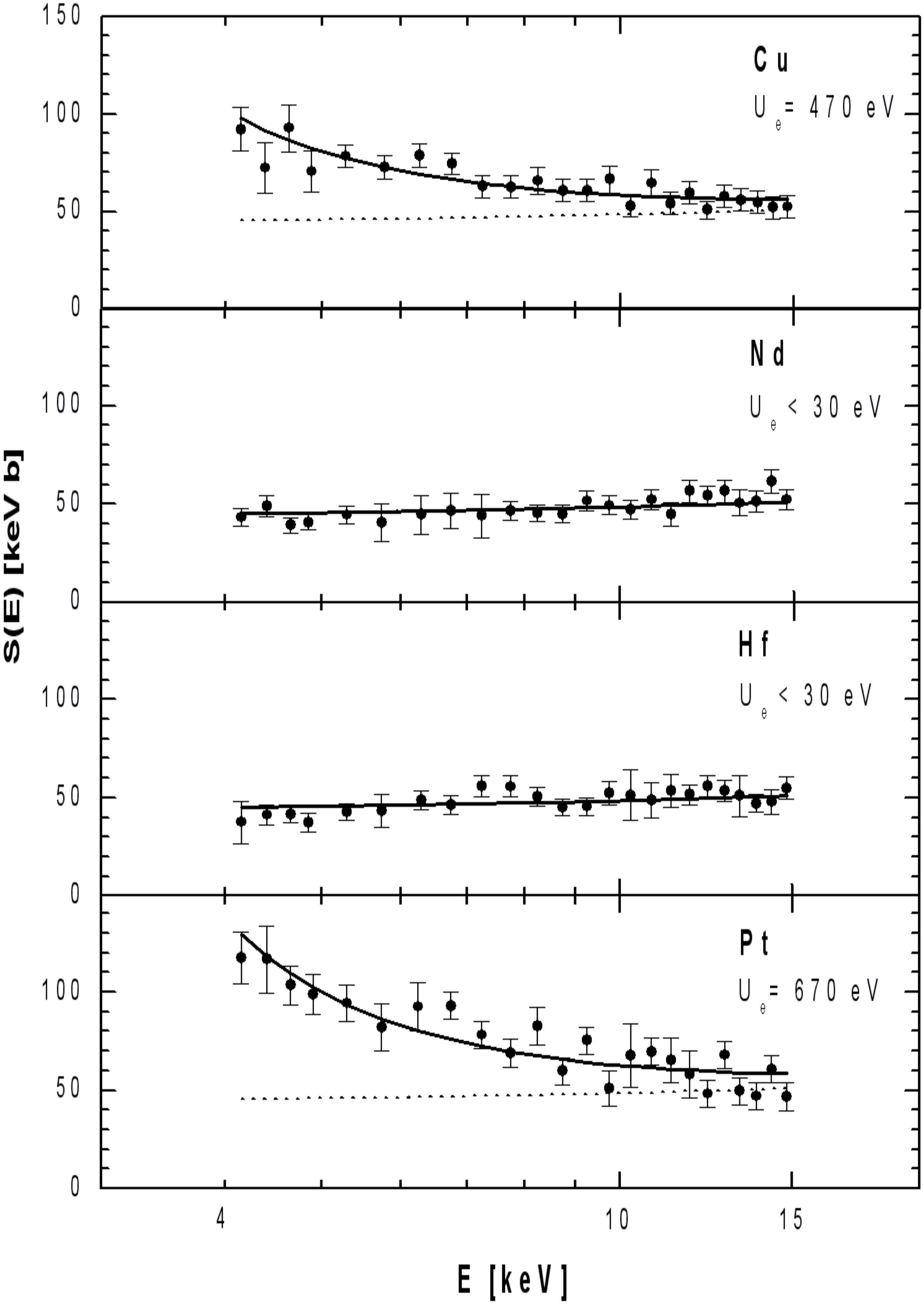
150
100
50
0
Cu
U_e = 470 eV
Nd
U_e < 30 eV
Hf
U_e < 30 eV
Pt
U_e = 670 eV
S(E) [keV b]
4
10
15
E [keV]

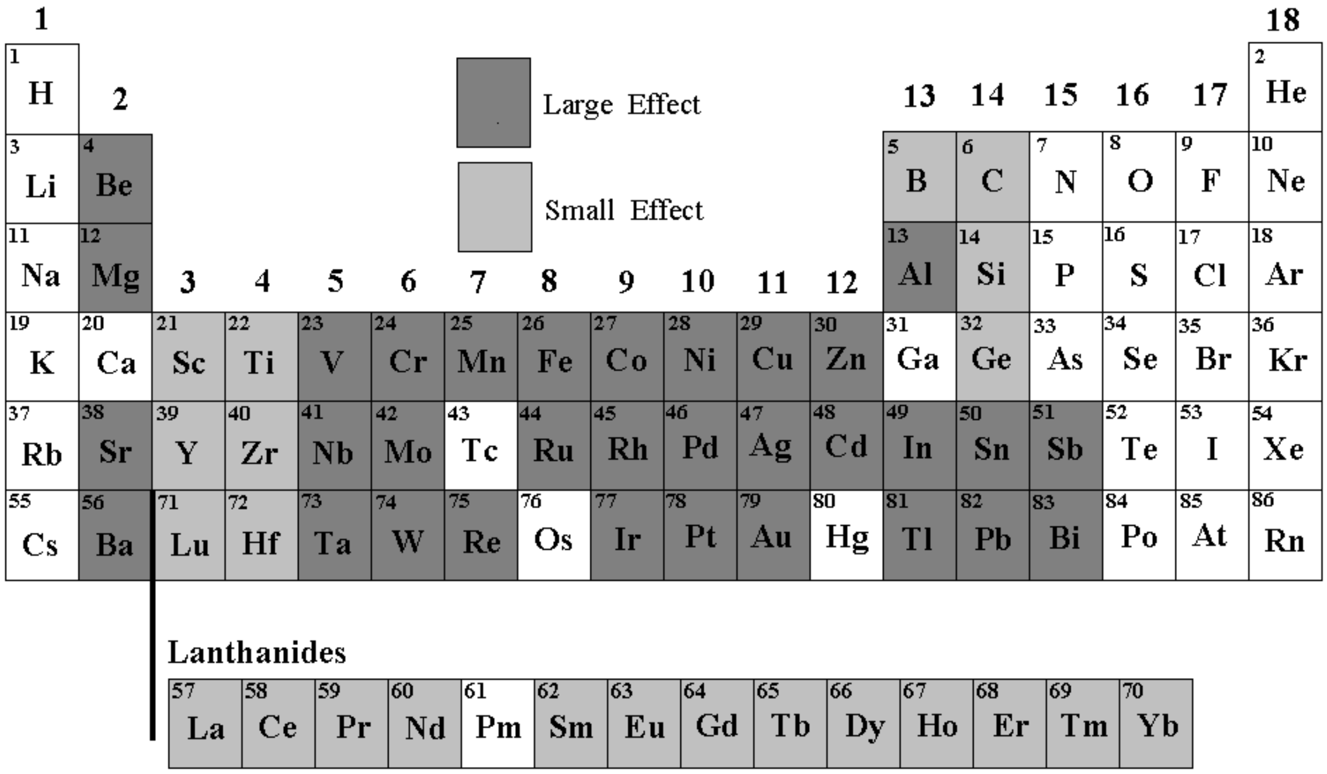

▓ Large Effect

░ Small Effect

1	2	3	4	5	6	7	8	9	10	11	12	13	14	15	16	17	18
1 H																	2 He
3 Li	4 Be ▓											5 B ░	6 C ░	7 N	8 O	9 F	10 Ne
11 Na	12 Mg ▓											13 Al ▓	14 Si ░	15 P	16 S	17 Cl	18 Ar
19 K	20 Ca	21 Sc ░	22 Ti ░	23 V ▓	24 Cr ▓	25 Mn ▓	26 Fe ▓	27 Co ▓	28 Ni ▓	29 Cu ▓	30 Zn ▓	31 Ga	32 Ge ░	33 As	34 Se	35 Br	36 Kr
37 Rb	38 Sr ▓	39 Y ░	40 Zr ░	41 Nb ▓	42 Mo ▓	43 Tc	44 Ru ▓	45 Rh ▓	46 Pd ▓	47 Ag ▓	48 Cd ▓	49 In ▓	50 Sn ▓	51 Sb ▓	52 Te	53 I	54 Xe
55 Cs	56 Ba ▓	71 Lu ░	72 Hf ░	73 Ta ▓	74 W ▓	75 Re ▓	76 Os	77 Ir ▓	78 Pt ▓	79 Au ▓	80 Hg	81 Tl ▓	82 Pb ▓	83 Bi ▓	84 Po	85 At	86 Rn

Lanthanides

57 La ░	58 Ce ░	59 Pr ░	60 Nd ░	61 Pm	62 Sm ░	63 Eu ░	64 Gd ░	65 Tb ░	66 Dy ░	67 Ho ░	68 Er ░	69 Tm ░	70 Yb ░